Preliminary CFD Analysis on Subcooled Boiling Flow under the Low-pressure Conditions

Su-Yeon Hyeon [a], Yeon-Gun Lee [a]*

aDept. of Nuclear and Energy Engineering, Jeju National Univ., #66 Jejudaehakno, Jeju-si, Jeju, KOREA
Corresponding author: yeongun2@jejunu.ac.kr

1. Introduction

Although the liquid temperature doesn't reach the saturation temperature, the boiling phenomena may occur near the heater surface, which has higher temperature than the liquid saturation temperature. This is called the subcooled boiling flows. It is one of important phenomena for a nuclear power plant(NPP) operation and safety. The generated bubbles near the heated surface by boiling influence the heat transfer characteristic and the pressure drop in systems [1]. Most PWRs operate at about 15.5 MPa, and therefore many studies have focused on flow boiling at high-pressure conditions [2-4].

For the above reasons, existing CFD (Computational Fluid Dynamics) codes have mostly used the model developed at high-pressure conditions for subcooled boiling phenomena. There is the difference of thermal-hydrodynamic characteristics at low-pressures from those at high-pressures (ex. behavior of vapor bubbles, density of liquid and vapor etc.). Therefore, it is not appropriate to directly apply the same models on major parameters both to high-pressure and to low-pressure conditions [4,5]. Thus, it is required to improve the capability of prediction on the low-pressure subcooled boiling flows. In this study, subcooled boiling experiments were analyzed using a commercial CFD code, ANSYS-CFX 17.2, that adopts the heat partition model for the wall boiling model. The experiments for simulation includes those conducted at high- and low-pressure conditions. The predicted distribution of the void fraction are compared with the experiment results.

2. CFD model for subcooled boiling flow

2.1 The wall boiling model

Kurul and Podowski(1990) proposed the heat partition model for subcooled boiling phenomena, which is the basic model for CFD simulation on the wall boiling. ANSYS CFX code has adapted this model, so-called RPI model. In heat partition model, the total heat flux, applied to the heated wall is composed of three parts :

$$Q_w = Q_c + Q_e + Q_q \qquad (1)$$

where Q_c, Q_e and Q_q denote the heat flux components due to single-phase turbulent convection, evaporation, and quenching, respectively [6].

In PRI model, the whole wall is composed of two fraction as shown in Eq.(2),

$$A_1 + A_2 = 1. \qquad (2)$$

A_2 and A_1 represent the fraction of area influenced by the bubbles and the rest of the wall surface, respectively. Therefore, there are no bubbles in A_1.

For the single-phase, the heat flux by the single-phase turbulent convection is as follows,

$$Q_c = A_1 h_c (T_w - T_l), \qquad (3)$$

where T_w, T_l and h_c are the wall temperature, the liquid temperature and the turbulence heat transfer coefficient [7].

In fraction A_2, the evaporation heat transfer takes place, and contributes to evaporation of the subcooled fluid. The evaporation heat flux, Q_e, can be calculated by,

$$\dot{Q}_e = m(h_{g,sat} - h_l), \qquad (4)$$

where $h_{g,sat}$ and h_l are the specific enthalpies of the saturated vapor and subcooled liquid, respectively.

The evaporation mass transfer rate is

$$\dot{m} = \frac{\pi d_w^3}{6} \rho_g fn. \qquad (5)$$

d_w, ρ_g, f and n are the bubble departure diameter, the density of the vapor, the bubble departure frequency and the density of active nucleation sites, respectively.

After a bubble departs, the single-phase liquid will contact with the heated wall. Until the next bubble formation, a thermal transient conduction takes place at the fraction of A_2 [2]. This mechanism of heating the liquid phase is called quenching, and is modeled as [7],

$$Q_q = A_2 h_q (T_w - T_l), \qquad (6)$$

where h_q is the quenching heat transfer coefficient and given by,

$$h_q = \left(\frac{2}{\sqrt{\pi}}\right) f \sqrt{t_w k_l \rho_l C_{Pl}}, \qquad (7)$$

where t_w, k, ρ, C_p and the subscript l denote the waiting time of bubbles, the thermal conductivity, the density, the specific heat at a constant pressure and the liquid phase.

There are various sub-models related on these parameters for the heat partition model. It is the key to apply the appropriate sub-models to improve the prediction capability of subcooled boiling flows. In this study, the subcooled boiling experiments at low- and high-pressures were simulated using the ANSYS-CFX code. The default models for major parameters adopted in this code are summarized in Table 1.

Table 1: Major parameters for heat partition model of ANSYS-CFX code [7]

Parameter	Model
Active nucleate site density, n	Lemmert and Chwala(1977) $n = \left[210 \left(T_w - T_l \right) \right]^{1.805}$
Bubble departure frequency, f	Kurul and Podowski(1970) $f = \sqrt{\dfrac{4g\left(\rho_l - \rho_g\right)}{3 C_D d_w \rho_l}}$ C_D : surface tension coefficient
Bubble departure diameter, d_w	Tolubinsky and Kostanchuk(1970) $d_w = \min\left(0.0006 e^{-\frac{T_{sat} - T_l}{45}}, 0.0014 \right)$ T_{sat} : saturation temperature
Bubble waiting time, t_w	Tolubinsky and Kostanchuk(1970) $t_w = \dfrac{0.8}{f}$
Area influence factor, F	Kurul and Podowski(1990) $F = 2$

2.2 CFD simulation of subcooled boiling experiments

2.2.1 High-pressure experiments

Bartolomey's [8] and Christensen's [9] tests were simulated for the subcooled boiling tests at high-pressure conditions. The test section of Bartolomey's experiment is a cylindrical channel with the inner diameter of 0.154 m and the heated length of 2 m. Before the simulation, mesh optimization, to find the minimum mesh number over which the void fraction no longer varies as the node refined, was performed [9]. Consequently, a total mesh number of 4,650 was applied.

The test section of Christensen's experiments is a rectangular channel (0.0111 m × 0.0444 m × 1.270 m). The total mesh number is 22,500. The mesh of ANSYS-CFX code is presented in Fig. 1.
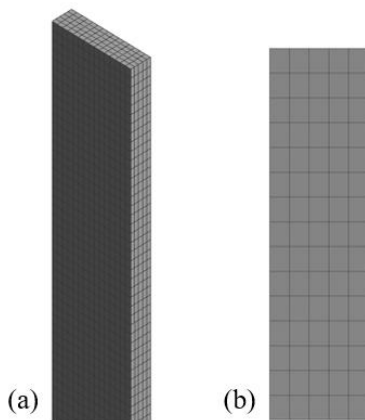
Fig. 1. The mesh for Christensen's test of ANSYS-CFX code; (a) side view (b) top view

2.2.2 Low-pressure experiments

For the low-pressure experiments, SUBO [10] and Jeju National University(JNU) tests are simulated using the ANSYS-CFX code. The test section of the SUBO test consists of a vertical cylindrical channel with a heater rod. The test section is 0.0355 mm in inner diameter, and 3.883 m in effective length. The outer diameter of heater is 0.00998 m. In this test, double sensor optical probes have been applied to measure the parameters of local bubbles [10]. As the result of mesh optimization, the total mesh number of 240,000 were used for the SUBO geometry.

The test section of the JNU test consists of a vertical cylindrical channel with a heater rod. The test section is 0.03 m in inner diameter, and 2 m in effective length. The outer diameter of heater is 0.01 m. For measurements of propagation of the radial void fractions, optical probes were used. The heated section was simulated such as the SUBO case. The total mesh number of 125,000 was decided by the mesh optimization for the JNU geometry. The mesh of ANSYS-CFX code is presented in Fig. 2. In this case, the turbulence model adapted the SST(Shear Stress Transport) model.
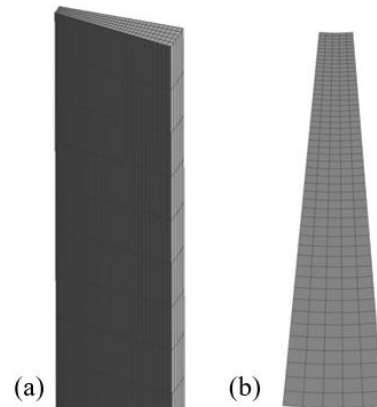
Fig. 2. The mesh for JNU test of ANSYS-CFX code; (a) side view (b) top view

3. Results and Discussion

3.1 Results at high-pressure conditions

The calculated void fraction is compared with the experiment results in Figs. 3 and 4. The x-axis indicates the normalized distance from the inlet, and the y-axis is the area-averaged void fraction.

The predictions of the void fraction distribution are in good agreement with the measurements. The calculated results are slightly over-estimated. However, the standard error is small enough to be within 26%. The ANSYS-CFX code reproduce well the bubble generation rate and the corresponding mean void fraction on high-pressure experiments.
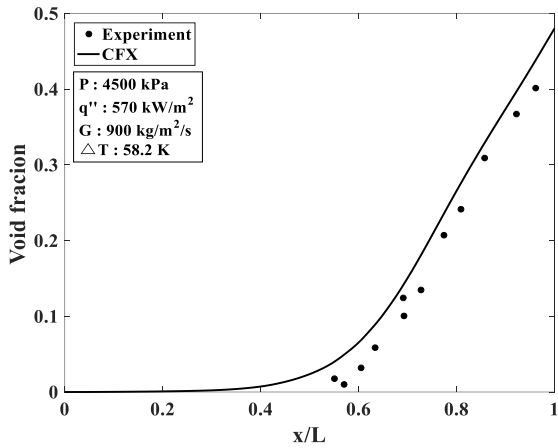
Fig. 3. Comparison of ANSYS-CFX and experiments for void fraction; Bartolomey's test
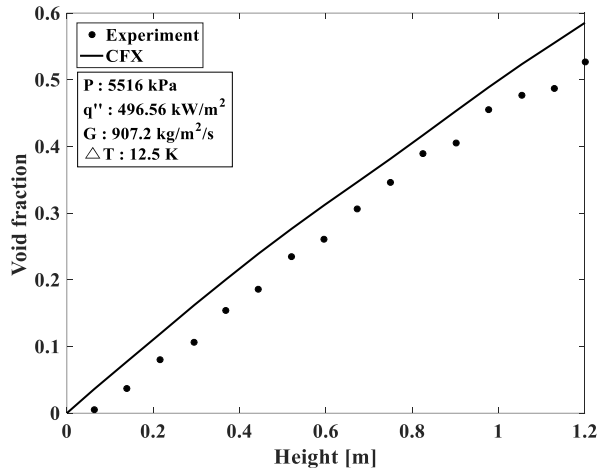
Fig. 4. Comparison of ANSYS-CFX and experiments for void fraction; Christensen's test

3.2 Results at low-pressure conditions

The comparison of simulational and experimental results for the local void fraction is represented in Figs. 5 and 6. The marks are experiment data and lines are calculated results. The x-axis is r^*, which is a dimensionless radial position.

$$r^* = \frac{(r - r_i)}{(r_o - r_i)} \tag{8}$$

In the SUBO test, the void fraction distribution along the radial and axial direction does not match to measurement data. It results from the use of the default models for major parameters, which is mostly validated at high-pressures, in ANSYS-CFX. Furthermore, bubbles spread all over the channel in experiments. But, vapor bubbles exist only near the heated surface in simulation results.

The calculated radial void fraction profile of the JNU test also deviates a lot from the measurement data. Bubbles are concentrated near the heated surface, such as

the SUBO result. Besides, the void fraction in L/D_h=21.5 is higher than in L/D_h=46.5. However, in experiments, the void fraction is higher in L/D_h=21.5 than in L/D_h=42.5 only near the heated surface, so it shows a different tendency from the measured data. It does not adequately predict the distribution of the void fraction along the axial direction. Therefore, sub-models for major parameters in the RPI model should be selected appropriately to improve the prediction for low-pressures. Furthermore the distribution of the radial void fraction is affected not only by the bubble mean diameter, but by non-drag forces for the interfacial momentum transfer, such as lift force, wall lubrication force, turbulent dispersion force and virtual mass force. Accordingly, the analysis on these forces is additionally necessary.
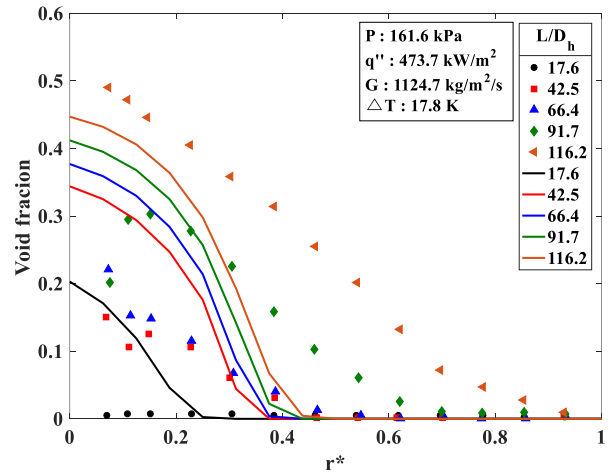
Fig. 5. Comparison of ANSYS-CFX and experiments for void fraction; SUBO test
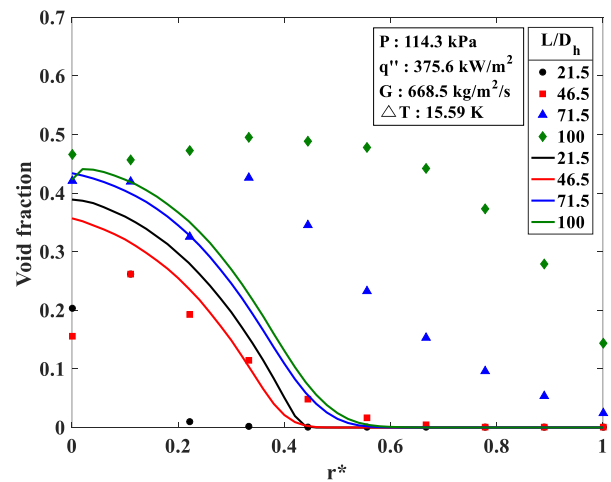
Fig. 6. Comparison of ANSYS-CFX and experiments for void fraction; JNU test

4. Conclusions

In this study, subcooled boiling experiments at high- and low-pressures are simulated using a commercial code, ANSYS-CFX. The predictions of void fraction profile show good agreement with measured data at high-pressure experiments. On the other hand, at low-pressure conditions, the distribution of void fraction is not well predicted. In simulations of both experiments, SUBO and JNU tests, bubbles are concentrated near the heated surface. Therefore, it needs appropriate selection of sub-models for the RPI model, such as the bubble departure diameter and a nucleate site density. Additional validations for the bubble mean diameter and the non-drag forces are also required.

ACKNOWLEDGMENTS

REFERENCES

[1] Ba-Ro Lee, Yeon-Gun Lee, Numerical Study of Low-pressure Subcooled Flow Boiling in Vertical Channels Using the Heat Partitioning Model, Tans. Korean Soc. Mech. Eng. B, Vol. 40, pp. 457-470, 2016

[2] J.Y. Tu, G.H. Yeoh, On numerical modelling of low-pressure subcooled boiling flows, Int. J. Heat Mass Transfer, Vol. 45, pp. 1197-1209, 2002

[3] Yong-Seok Choi, You-Taek Kim, Tae-Woo Lim, CFD validation for subcooled boiling under low pressure, J. Korean Soc. Of Marine Engineering(JKOSME), Vol. 40, No. 4, pp. 275-281, 2016

[4] Boštjan Končar, Borut MavKo, CFD SIMULATION OF SUBCOOLED FLOW BOILING AT LOW PRESSURE, Proceedings of International Conference Nuclear Energy in Central Europe, September, pp. 10-13, 2001

[5] Boštjan Končar, Ivo Kljenak, Borut Mavko, Modelling of local two-phase flow parameters in upward subcooled flow boiling at low pressure, Int. J. Heat Mass Transfer, Vol. 47, pp.1499-1513, 2004

[6] Eckhard Krepper, Roland Rzehak, CFD for subcooled flow boiling: Simulation of DEBORA experiments, Nucl. Eng. Des., Vol. 241, pp. 3851-3866, 2011

[7] ANSYS, Inc., ANSYS CFX-Solver Theory Guide, 2012

[8] D. Shaver, M. Podowski, Modeling and Validation of Forced Convection Subcooled Boiling, Proc. 16th Int. Topical Meeting on Nuclear Reactor Thermalhydraulics(NURETH-16), 2015

[9] Ba-Ro Lee, Yeon-Gun Lee, Numerical study of subcooled boiling phenomena using a component analysis code, CUPID, Transactions of the Korean Nuclear Society, October, 2015

[10] B.J. Yun, B.U. Bae, D.J. Euh, G.C. Park, C.H. Song, Characteristics of the local bubble parameters of a subcooled boiling flow in an annulus, Nucl. Eng. Des., Vol. 240, pp. 2295-2303, 2010